DYNAMIC POST-BUCKLING ANALYSIS OF THE MICRO-FOLDING Augusti 3D MODEL WITH LOCAL SYMMETRY-BREAKINGS

I. Ario[1] and M. Nakazawa[2]
[1]*Dept. of Civil & Environmental Engineering, Hiroshima University*
E-mail: mario@hiroshima-u.ac.jp

[2]*Dept. of Civil & Environmental Engineering, Tohoku-Gakuin University*
E-mail: naka@tjcc.tohoku-gakuin.ac.jp

Keywords: Bifurcation Analysis, Postbuckling, Multi Folding, Snap-through Behaviour.

This paper reviews the theoretical basis for the dynamic numerical analysis to examine the elastic stability of a folding multi-layered truss [1]. The analysis allows for geometrical non-linearity and contact between nodes and is based upon bifurcation theory [2]. Comparisons are made between experimental folding patterns and the patterns obtained from the numerical method in which bifurcations are demonstrated as elastic unstable snap-through behaviour (e.g. [3]). In this paper, the bifurcation behavioural characteristics of a cone and diamond-shaped axisymmetric space truss made of 4×2 elastic members with 4-directional symmetry are studied as folding mechanism in three dimension space. Equilibrium equations of the truss are investigated using a transformation matrix based on group theory in mathematics. The equilibrium equations show bifurcation points and paths by the vanishing of lower-order terms, resulting in non-vanishing terms with higher-order nonlinearity. The geometric symmetry of the truss results in a symmetrical up-down deformation at a critical singular point for this simplified model.

The authors suggest that the understanding of snapthrough behaviour for folding mechanics in three-dimensional space will be very useful for the development of lightweight structures subject to bifurcation of the hill-top branching type.

1 Introduction

Folding the weight of a structure from the viewpoint of the first critical load of the perfect structure usually produces a design for which the critical loads for several buckling modes coincide. This causes interaction of buckling modes in which the multiplier multiplies α^m is increased or the exponent m is decreased [4, 5]. To discover the finding out multiple bifurcation point as the critical load in theoretical folding mechanics, a method for obtaining the bifurcation paths of a discreted structural system with nonlinear equilibrium equations has been studied by Ario et al. In these papers, they referred to the hill-top-bifurcation behaviour of a three-layer plane truss subjected to a vertical loading at the top node. A comment is also given without any proof for the existence of an infinite number of multiple snap-through behaviors for a multiple-layered pantograph truss system. And the hill-top bifurcation and bifurcation paths also for the system. We are more interested in a system which is made of three-dimensional space even though it is a simple model because there might be more complex and strange phenomena in nonlinear mechanics. Thus, higher geometric symmetry tends to yield a greater number of bifurcation paths.

This paper aimes to investigate the bifurcation behaviour of the axisymmetric space diamond truss shown in **Fig.4**. We want to know why there are more interesting bifurcation paths for this diamond space truss. The bifurcation behaviour of a diamond space truss is studied as a simplified

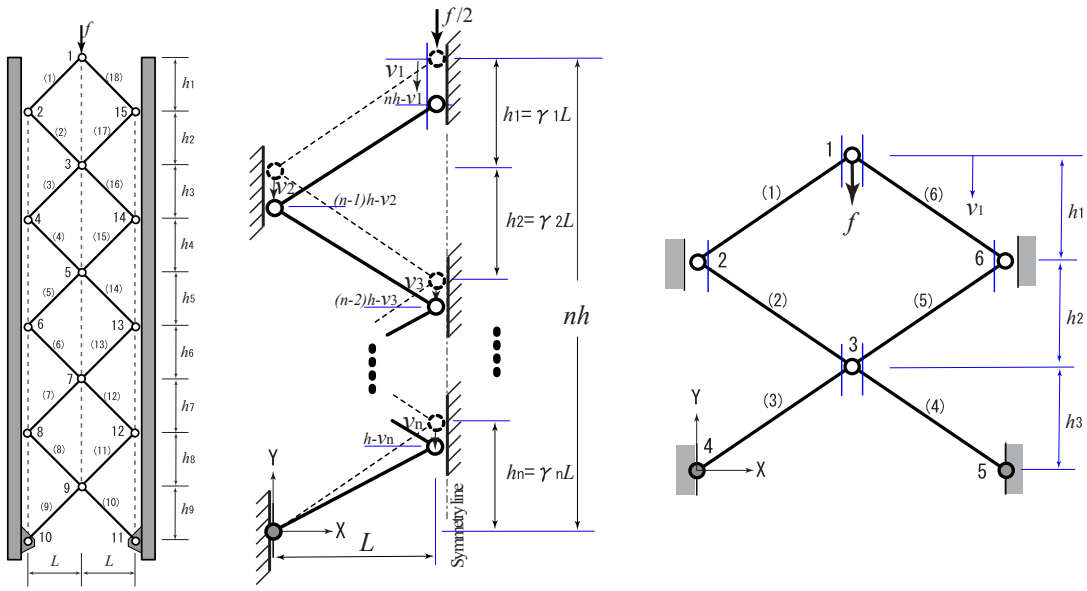

Figure 1: Multi-folding pantographic systems; (a) Multi-layer model, (b) One half of multi-layer model, (c) Basic 3 layer model

folding model. Since the main object of this paper is the study of the bifurcation behaviour of an axisymmetric truss, the Euler buckling of each member is disregarded, i.e., it is assumed as not to occur.

2 Theory of Elastic Folding

In this section, we consider the folding mechanisms for the three layer truss structure subject to a vertical impact load at the top node shown in Fig. 1(c). The system is a pin-jointed elastic truss and all nodes of the system displace vertically only. No allowance is made for friction or gravity for this geometrically nonlinear problem.

2.1 Theoretical approach for multi-folding truss on 2D

We assume a periodic height for each layer of $h_i = \gamma_i L$ where the width L of the truss is fixed. Therefore, an initial length for each bar in the geometry of the figure is expressed as

$$\ell_i = \sqrt{L^2 + h_i^2} = L\sqrt{1 + \gamma_i^2}, \quad \text{for } i = 1, \cdots, n. \tag{1}$$

The deformed length of each bar denoted as $\hat{\ell}_i$, is a function of the height and the nodal displacement variables

$$\begin{aligned} \hat{\ell}_1 &= \sqrt{L^2 + \{(nh - v_1) - ((n-1)h - v_2)\}^2} \\ &= L\sqrt{1 + (\gamma_1 - \bar{v}_1 + \bar{v}_2)^2}\,, \end{aligned} \tag{2}$$

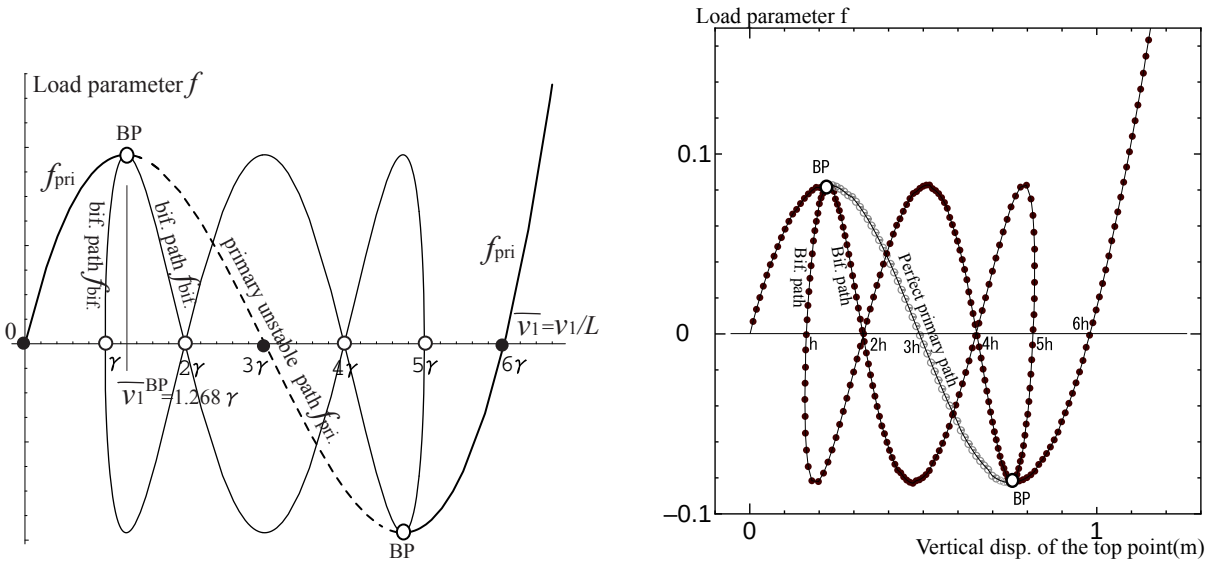

(a) (b)

Figure 2: Static equilibrium paths without contact for the basic model; (a) Theoretical equilibrium paths using Eqs.(23) and (24), (b) Numerical static equilibrium paths

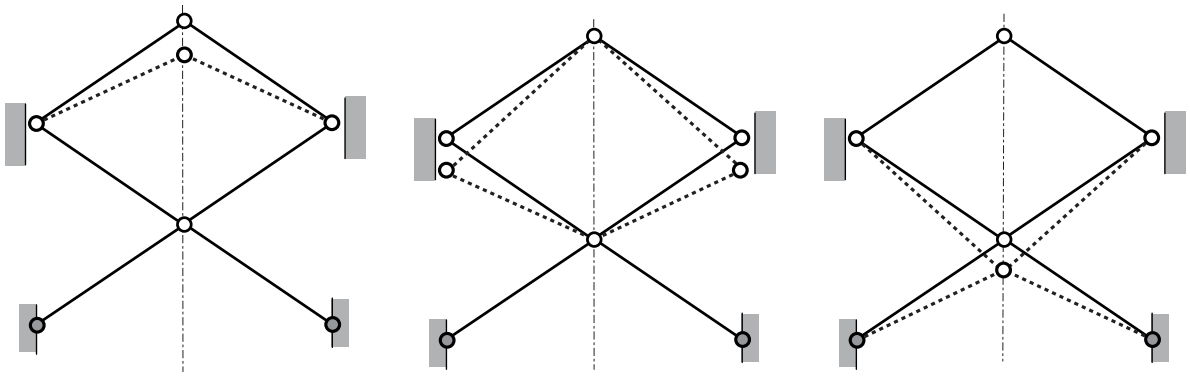

(a) (b) (c)

Figure 3: Nodal displacement initiating fold mode; (a) the top members folding mode as $\boldsymbol{\eta}_1$, (b) the middle members folding mode as $\boldsymbol{\eta}_2$, (c) the bottom members folding mode as $\boldsymbol{\eta}_3$

$$\vdots$$

$$\hat{\ell}_i = L\sqrt{1+(\gamma_i-\bar{v}_i+\bar{v}_{i+1})^2}\,, \tag{3}$$

$$\vdots$$

$$\hat{\ell}_n = L\sqrt{1+(\gamma_n-\bar{v}_n)^2} \tag{4}$$

where $\gamma_i = h_i/L > 0, \quad \bar{v}_i = v_i/L, \quad (i = 1, \cdots, n)$ and $\bar{v}_{n+1} = 0$ because the bottom node is translationally fixed.

Using Green's expression for strain (see Appendix A for engineering strain formulation) we obtain the elastic strain in each bar as

$$\varepsilon_i \equiv \frac{1}{2}\left\{\left(\frac{\hat{\ell}_i}{\ell_i}\right)^2 - 1\right\}, \quad \text{for } i = 1, \cdots, n. \tag{5}$$

Substituting Eq.(25) to Eq.(4) into Eq.(5) we obtain

$$\varepsilon_i = \frac{1}{2}\left\{\frac{1+(\gamma_i-\bar{v}_i+\bar{v}_{i+1})^2}{1+\gamma_i^2} - 1\right\}, \quad \text{for } i = 1, \cdots, n. \tag{6}$$

The total potential energy, $\mathcal{V}$, of the half model, subject to loading $f/2$ is then given by

$$\mathcal{V} = \sum_{i=1}^{n} \frac{EA_i\ell_i}{2}(\varepsilon_i)^2 - \frac{f}{2}\bar{v}_1 L \tag{7}$$

$$= \sum_{i=1}^{n} \frac{EA_iL\sqrt{1+\gamma_i^2}}{2}\frac{1}{4}\left\{\frac{1+(\gamma_i-\bar{v}_i+\bar{v}_{i+1})^2}{1+\gamma_i^2} - 1\right\}^2 - \frac{f}{2}\bar{v}_1 L. \tag{8}$$

For the case when $\gamma_i = \gamma, \ (i = 1, \cdots, n)$ and $EA_i = EA, \ (i = 1, \cdots, n)$ the total potential energy can be written as

$$\mathcal{V} = \frac{\beta L}{8}\sum_{i=1}^{n}(\bar{v}_i - \bar{v}_{i+1})^2\left((\bar{v}_i - \bar{v}_{i+1}) - 2\gamma\right)^2 - \frac{f}{2}\bar{v}_1 L \tag{9}$$

where the stiffness parameter $\beta = EA/(1+\gamma^2)^{3/2}$ (i.e. β is a function of γ). From Eq. (9), we can obtain the equilibrium equations based on the principal of minimum energy [4] in the following way:

$$F_i(\cdots, v_i, \cdots) \equiv \frac{\partial \mathcal{V}}{\partial v_i} = \frac{\partial \mathcal{V}}{\partial \bar{v}_i}\frac{\partial \bar{v}_i}{\partial v_i} = 0\,, \quad \text{for } i = 1, \cdots, n. \tag{10}$$

Hence, for the 1st, $i-$th and $n-$th equilibrium equations are

$$F_1(\bar{v}_1, \bar{v}_2) = \frac{\beta}{2}(\bar{v}_1 - \bar{v}_2)((\bar{v}_1 - \bar{v}_2) - \gamma)((\bar{v}_1 - \bar{v}_2) - 2\gamma) - \frac{f}{2} = 0\,, \tag{11}$$

$$F_i(\bar{v}_{i-1}, \bar{v}_i, \bar{v}_{i+1}) = (\bar{v}_{i-1} - \bar{v}_i)((\bar{v}_{i-1} - \bar{v}_i) - \gamma)((\bar{v}_{i-1} - \bar{v}_i) - 2\gamma)$$
$$-(\bar{v}_i - \bar{v}_{i+1})((\bar{v}_i - \bar{v}_{i+1}) - \gamma)((\bar{v}_i - \bar{v}_{i+1}) - 2\gamma) = 0\,, \tag{12}$$

$$F_n(\bar{v}_{n-1}, \bar{v}_n) = (\bar{v}_{n-1} - \bar{v}_n)((\bar{v}_{n-1} - \bar{v}_n) - \gamma)((\bar{v}_{n-1} - \bar{v}_n) - 2\gamma)$$
$$-\bar{v}_n(\bar{v}_n - \gamma)(\bar{v}_n - 2\gamma) = 0\,. \tag{13}$$

By using the implicit function theorem it is then possible to solve for all variables $\bar{v}_i$, $(i = n, \cdots, 1)$ as follows

$$\begin{aligned} F_n(\bar{v}_{n-1}, \bar{v}_n) &= 0 \rightarrow \bar{v}_n = \mathcal{F}_n(\bar{v}_{n-1}) \,, & (14)\\ F_i(\bar{v}_{i-1}, \bar{v}_i, \bar{v}_{i+1}) = F_i(\bar{v}_{i-1}, \bar{v}_i, \mathcal{F}_{i+1}(\bar{v}_i)) &= 0 \rightarrow \bar{v}_i = \mathcal{F}_i(\bar{v}_{i-1}), & (15)\\ F_1(\bar{v}_1, \bar{v}_2) = F_1(\bar{v}_1, \mathcal{F}_2(\bar{v}_1)) &= 0 & (16) \end{aligned}$$

where $\mathcal{F}(\cdot)$ denotes a nonlinear function. Thus we obtain all the solutions for each nonlinear equilibrium path by finding the normalised nodal displacements in turn.

The stability of the system is given by a non zero value for the determinant of the tangent stiffness matrix, the *Jacobian* for $J \in \mathbf{R}^{n\times n}$. J is defined as follows:

$$J \equiv (J_{ij}) = \left(\frac{\partial^2 \mathcal{V}}{\partial v_i \partial v_j}\right) = \left(\frac{\partial^2 \mathcal{V}}{\partial \bar{v}_i \partial \bar{v}_j}\frac{\partial \bar{v}_i}{\partial v_i}\frac{\partial \bar{v}_j}{\partial v_j}\right) = \left(\frac{\partial F_i}{\partial \bar{v}_j}\frac{\partial \bar{v}_j}{\partial v_j}\right), \quad \text{for } i, j = 1, \cdots, n \qquad (17)$$

and instability is defined as

$$\det J(v_i) = 0 \,. \qquad (18)$$

It is then possible to determine the buckling load and the post-buckling mode shape of the truss at the singular points from the nonlinear equations during instability.

2.2 Bifurcation analysis for three layers model ($n = 3$)

We now determine the equilibrium paths for the basic model shown in Fig. 1(c). The height of each layer is identical, i.e. $h_i = h$, hence $\gamma_i = \gamma$. In order to solve for the variable $\bar{v}_i$, we use the implicit function theorem and substitute $n = 3$ into Eqs.(13) and (14) which gives the solutions as follows:

$$\bar{v}_3 = \mathcal{F}_3(\bar{v}_2) \begin{cases} = \bar{v}_2/2 & \text{for primary path,} \\ = \frac{1}{2}\left(\bar{v}_2 \pm \sqrt{-3\bar{v}_2^2 + 12\gamma\bar{v}_2 - 8\gamma^2}\right) & \text{for bif. paths,} \end{cases} \qquad (19)$$

$$\bar{v}_2 = \mathcal{F}_2(\bar{v}_1) \begin{cases} = 2\bar{v}_1/3 & \text{for primary path,} \\ = -\gamma + \bar{v}_1 \pm \frac{\sqrt{3}}{3}\sqrt{-(\bar{v}_1 - \gamma)(\bar{v}_1 - 5\gamma)} & \text{for bif. paths.} \end{cases} \qquad (20)$$

The use of the implicit function theorem (16) and/or (11) for $\bar{v}_1$ leads to the following equation:

$$F_1\left(\bar{v}_1, \mathcal{F}_2(\bar{v}_1)\right) = f - \beta\mathcal{F}_1(\bar{v}_1) = 0 \qquad (21)$$

hence it is seen that the relationship between the load parameter and the displacement $\bar{v}_1$ is nonlinear

$$f = \beta\, \mathcal{F}_1(\bar{v}_1). \qquad (22)$$

Using $\bar{v}_2 = \mathcal{F}_2(\bar{v}_1)$ and $\bar{v}_3 = \mathcal{F}_3(\bar{v}_2)$ we can then express the equilibrium equations for the primary and bifurcation paths in terms of variable $\bar{v}_1$ as follows

$$\begin{aligned} f_{\text{pri.}} &= \beta\frac{\bar{v}_1}{3}\left(\frac{\bar{v}_1}{3} - \gamma\right)\left(\frac{\bar{v}_1}{3} - 2\gamma\right), \quad \text{for primary path,} & (23)\\ f_{\text{bif.}} &= \pm\frac{\beta}{3\sqrt{3}}\sqrt{-(\bar{v}_1 - \gamma)(\bar{v}_1 - 5\gamma)}\cdot(\bar{v}_1 - 2\gamma)(\bar{v}_1 - 4\gamma), \quad \text{for bif. paths} & (24) \end{aligned}$$

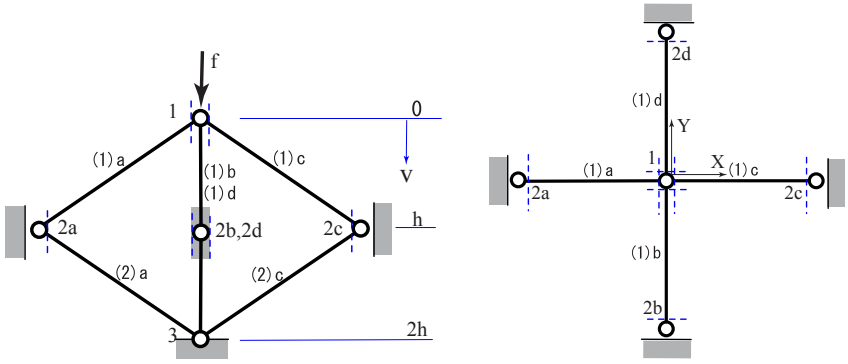

Figure 4: Folding model in 3D

The theoretical primary equilibrium and bifurcation paths are shown in Fig. 2(a). We obtain the critical positions for the truss using the condition $df/d\bar{v}_1 = 0$ for maximum and minimum values. For the equilibrium paths under consideration we obtain above the following result

$$\bar{v}_1^{\rm BP} = \frac{3 \mp \sqrt{3}}{3}(3\gamma) = (3 \mp \sqrt{3})\gamma = \left\{ \begin{array}{l} 1.268\gamma, \\ 4.732\gamma. \end{array} \right. , \quad \text{for } n = 3$$

Finally the maximum load is given by

$$f_{\max} = f(\bar{v}_1^{\rm BP}) = \pm \frac{2\gamma^3}{3\sqrt{3}}\beta.$$

3 Theoretical approach for multi-folding truss on 3D

We consider the folding mechanisms for a (pantographic) truss structure subject to a vertical impact load at the top node of the system shown in **Fig.4**. The system is a pin-jointed elastic truss and all nodes of the system displace vertically only. No allowance is made for friction or gravity for this geometrically nonlinear problem. And, we think that no Eular elastic buckling occurs for each bar by itself in this truss. We assume a periodic height for each layer of $h_i = \gamma_i L$ where the width L of the truss is fixed. Therefore, the initial length of each bar in the geometry of the figure is expressed as

$$\ell_{(i),k} = \sqrt{L^2 + h_i^2} = L\sqrt{1 + \gamma_i^2}, \quad \text{for } k = a, \cdots, d, \quad i = 1, 2. \tag{25}$$

Using a definition of the Green strain, the potential strain energy for the up and down side of this model, $\mathcal{V}_i$, of the model shown in **Fig.4**, subject to loading f^* is then given by

$$\mathcal{V}_1 = \frac{\beta L}{8} \sum_{k=a}^{d} \left(\bar{v}_1 - \bar{v}_{2,k}\right)^2 \left(\bar{v}_1 - \bar{v}_{2,k} - 2\gamma\right)^2, \tag{26}$$

$$\mathcal{V}_2 = \frac{\beta L}{8} \sum_{k=a}^{d} \left(\bar{v}_{2,k}\right)^2 \left(\bar{v}_{2,k} - 2\gamma\right)^2. \tag{27}$$

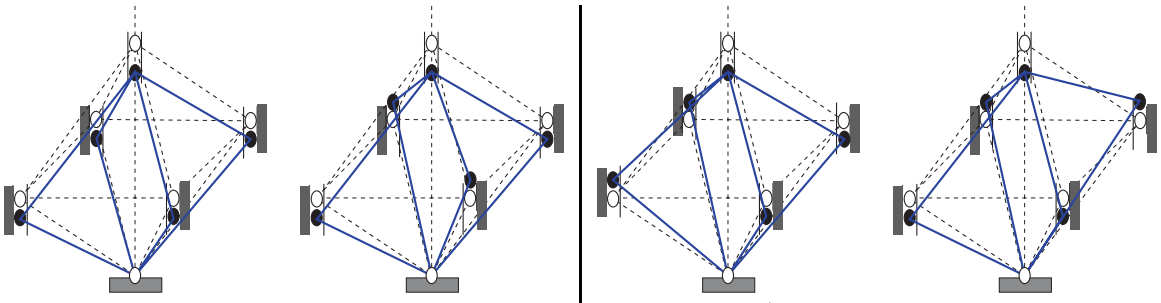

(a) $(1,1)_{D_4}$ (b) $(1,3)_{D_4}$ (c) $(2,1)^{+}_{D_4}$ (d) $(2,1)^{-}_{D_4}$

Figure 5: Deformation patterns for 3D folding model

Here, it is assumed, as the condition for this model $\beta = EA/(1+\gamma)^{3/2}, \gamma_i = \gamma, \bar{v}_i = v_i/L, h_i = h$. The total potential energy is expressed as follows;

$$\begin{aligned} \mathcal{V} &= \mathcal{V}_1 + \mathcal{V}_2 - f\bar{v}_1 L, & (28)\\ &= \frac{\beta L}{8}\sum_{k=a}^{d}\left[(\bar{v}_1 - \bar{v}_{2,k})^2(\bar{v}_1 - \bar{v}_{2,k} - 2\gamma)^2 + (\bar{v}_{2,k})^2(\bar{v}_{2,k} - 2\gamma)^2\right] - f\bar{v}_1 L & (29)\end{aligned}$$

We can obtain the equilibrium equations based on the principal of minimum energy in the following way:

$$F_i(\cdots, v_i, \cdots) \equiv \frac{\partial \mathcal{V}}{\partial v_i} = \frac{\partial \mathcal{V}}{\partial \bar{v}_i}\frac{\partial \bar{v}_i}{\partial v_i} = 0\ , \quad \text{for } i = 1, \cdots, n. \tag{30}$$

For example for $\bar{v}_1$, it is shown as

$$\begin{aligned} F_1 &= \frac{\partial \mathcal{V}}{L\bar{v}_1} = 0 & (31)\\ &= \frac{\beta}{4}\big\{(\bar{v}_1 - \bar{v}_{2a})^2(-2\gamma + \bar{v}_1 - \bar{v}_{2a}) + (\bar{v}_1 - \bar{v}_{2a})(-2\gamma + \bar{v}_1 - \bar{v}_{2a})^2\\ &\quad +(\bar{v}_1 - \bar{v}_{2b})(-2\gamma + \bar{v}_1 - \bar{v}_{2b})^2 + (\bar{v}_1 - \bar{v}_{2b})^2(-2\gamma + \bar{v}_1 - \bar{v}_{2b})\\ &\quad +(\bar{v}_1 - \bar{v}_{2c})(-2\gamma + \bar{v}_1 - \bar{v}_{2c})^2 + (\bar{v}_1 - \bar{v}_{2c})^2(-2\gamma + \bar{v}_1 - \bar{v}_{2c})\\ &\quad +(\bar{v}_1 - \bar{v}_{2d})(-2\gamma + \bar{v}_1 - \bar{v}_{2d})^2 + (\bar{v}_1 - \bar{v}_{2d})^2(-2\gamma + \bar{v}_1 - \bar{v}_{2d})\big\} - f = 0. & (32)\end{aligned}$$

The other shows

$$\begin{aligned} F_{2,k} &= \frac{\partial \mathcal{V}}{L\bar{v}_{2,k}} = 0, & (33)\\ &= \frac{\beta}{4}\big\{-(\bar{v}_1 - \bar{v}_{2,k})^2(-2\gamma + \bar{v}_1 - \bar{v}_{2,k}) - (\bar{v}_1 - \bar{v}_{2,k})(-2\gamma + \bar{v}_1 - \bar{v}_{2,k})^2\\ &\quad +\bar{v}_{2,k}^2(\bar{v}_{2,k} - 2\gamma) + \bar{v}_{2,k}(\bar{v}_{2,k} - 2\gamma)^2\big\} = 0. & (34)\end{aligned}$$

When it is subjected to the vertical load increasing at the top point of this model, this system has a critical load into elastic unstable state. Then, we might be able to foresee where there are several folding patterns in this system based on symmetry-breaking's law. The degree of freedom

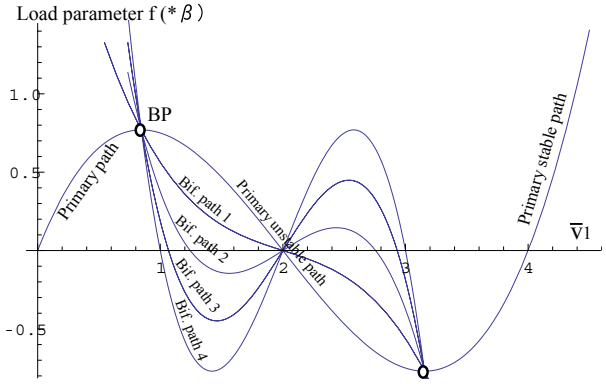

Figure 6: Primary path and bifurcation paths

of this system is limited to only the vertical displacement. As there is a displacement at the top node, large and strange deformations suddenly appear for four nodal points on the mid layer at the critical point. We can show that there are typical deformation patterns in a group representation of the dihedral group D_4 in the $Z-$ direction which is the irreducible representation space $\rho \in R(D_4)$ in the following:

$$\rho = \left\{(1,1)_{D_4}, (1,3)_{D_4}, (2,1)^{+}_{D_4}, (2,1)^{-}_{D_4}\right\}, \quad {}^{\forall}\rho \in R(D_4)$$

Here, there is the order of index as follows: the first $(1,*)_{D_4}$ and the second $(2,*)_{D_4}$. The second order of the symmetry means that there are a couple of representations as $+$, and $-$. The relationship between several deformed patterns of the system and the representation space is shown in **Fig.**5.

The theoretical solution for this equation is obtained by analytical work, as follows;

$$\bar{v}_{2,k} = \begin{cases} \frac{v_1}{2}, \\ \frac{1}{2}\left(\bar{v}_1 \pm \sqrt{-8\gamma^2 + 12\gamma\bar{v}_1 - 3\bar{v}_1^2}\right) \end{cases}, \qquad \text{for } k = a, b, c, d, \tag{35}$$

There are three solutions which include the linear and nonlinear term for each nodal displacement, $\bar{v}_{2,k}$. Therefore, it is considered that several equilibrium paths are combined by these chosen solutions. So, it is shown that there are a combination of linear and nonlinear solutions, such as "$\circ$" and "$\bullet$" shown in **Fig. 7**. This figure means there are a number of linear and nonlinear solutions for the nodal displacement, $\bar{v}_{2,k}$. For example, Figure (a) shows the marks of layout for four nodal points which correspond to the deformation pattern of the primary path, when the combination of all linear solution as $\bar{v}_{2,k} = \bar{v}_1/2$. Figures (b), (c), (d) and (e) are increasing the nonlinear solution for the points, the combination of all nonlinear solutions is shown in Figure (e), which corresponds to the deformation pattern of the 4-th bifurcation path. This equilibrium path is the most unstable state from the hill-top branch bifurcation, BP.

3.1 Primary path and bifurcation paths

In the previous subsection, we determined the three solutions for $\bar{v}_{2,k}$, and we can substitute them into the equilibrium equations $\boldsymbol{F}_i$. There are several equilibrium paths to be satisfied for the combination of these solutions. At first, if all displacements equal the same linear relationship

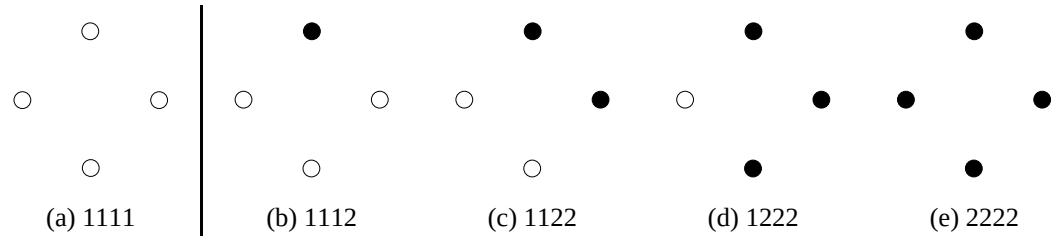

(a) 1111 (b) 1112 (c) 1122 (d) 1222 (e) 2222

Figure 7: Corresponding to a order of solutions('1' means the linear, '2' means the nonlinear solution to be substituted)

$\bar{v}_{2,k} = \bar{v}_1/2, (k = a, b, c, d)$ shown in **Fig. 7**(a), Eq.(32) will be the fundamental equilibrium equation as the primary path in the following:

$$f_{\text{pri.}} = \frac{\beta}{4}\bar{v}_1(\bar{v}_1 - 2\gamma)(\bar{v}_1 - 4\gamma). \tag{36}$$

This equation is the primary nonlinear path which has the D_4 symmetry of the same vertical displacements for $\bar{v}_{2,k}$. This deformation of the system is not symmetry-breaking of D_4, i.e. before D_4 symmetry-breaking.

At the second, we have got several bifurcation paths under the condition of solution's combination shown in **Fig. 7**(b) in the following:

$$\begin{aligned} \bar{v}_{2a} &= \bar{v}_{2b} = \bar{v}_{2c} = \bar{v}_1/2,\ \bar{v}_{2d} = \frac{1}{2}\left(\bar{v}_1 - \sqrt{-8\gamma^2 + 12\bar{v}_1\gamma - 3\bar{v}_1^2}\right) \\ f_{\text{bif.}} &= \frac{\beta}{16}\left(48\gamma^3 - 64v_1\gamma^2 + 30v_1^2\gamma - 5v_1^3\right), \quad \text{for bif. path 1.} \end{aligned} \tag{37}$$

Next, the condition of another combination of solutions including two nonlinear solutions, shown in **Fig.**7(c) is given as follows:

$$\begin{aligned} \bar{v}_{2a} &= \bar{v}_{2b} = \bar{v}_1/2,\ \bar{v}_{2c} = \bar{v}_{2d} = \frac{1}{2}\left(\bar{v}_1 - \sqrt{-8\gamma^2 + 12\bar{v}_1\gamma - 3\bar{v}_1^2}\right) \\ f_{\text{bif.}} &= \frac{\beta}{8}\left(48\gamma^3 - 80v_1\gamma^2 + 42v_1^2\gamma - 7v_1^3\right), \quad \text{for bif. path 2.} \end{aligned} \tag{38}$$

And, with an increasing number of nonlinear solutions for substituting into Eq.(32), there is one remaining linear relationship for $\bar{v}_{2,k}$;

$$\begin{aligned} \bar{v}_{2a} &= \bar{v}_1/2,\ \bar{v}_{2b} = \bar{v}_{2c} = \bar{v}_{2d} = \frac{1}{2}\left(\bar{v}_1 - \sqrt{-8\gamma^2 + 12\bar{v}_1\gamma - 3\bar{v}_1^2}\right) \\ f_{\text{bif.}} &= \beta\left(9\gamma^3 - 16v_1\gamma^2 + \frac{69{v_1}^2\gamma}{8} - \frac{23{v_1}^3}{16}\right), \quad \text{for bif. path 3.} \end{aligned} \tag{39}$$

Finally, Substituting all the nonlinear solutions into Eq.(32), we obtain the following relationship:

$$\begin{aligned} \bar{v}_{2a} &= \bar{v}_{2b} = \bar{v}_{2c} = \bar{v}_{2d} = \frac{1}{2}\left(\bar{v}_1 - \sqrt{-8\gamma^2 + 12\bar{v}_1\gamma - 3\bar{v}_1^2}\right) \\ f_{\text{bif.}} &= 2\beta\left(6\gamma^3 - 11v_1\gamma^2 + 6v_1^2\gamma - v_1^3\right), \quad \text{for bif. path 4} \end{aligned} \tag{40}$$

These relationships are plotted in **Fig.**6 as bifurcation paths from the first BP. We know that there are several different unstable paths during two BPs. The loss of the load parameter from BP depends on the number of nonlinear solutions as '•', i.e. when all solutions are linear and there are no nonlinear ones, it corresponds to the primary unstable path; on the other hand, when all solutions are nonlinear with no linear ones it corresponds to the most decreasing unstable bifurcation path (Bif. path 4 in **Fig. 6**). It is understood that there are several different bifurcation paths in the unstable area between one BP (hill-top) and the next BP (hill-bottom) for this simple model in three dimensions. All paths go through the center position $\bar{v}_1 = 2$. We realise that if one of these relationships is obtained from experimental data, as the result there will be a bifurcation path and a number of bifurcation solutions which depend on the influence of the lost load resistance.

4 Dynamic Analysis

It is well known that dynamic analysis and techniques with numerical work also, and for example, a simple truss [6] has one of strange attractor models of nonlinear dynamics. The dynamic analysis equation for the folding truss combines mass, damping and nonlinear stiffness $\{F_i(\boldsymbol{v})\}^{\mathrm{T}} = \boldsymbol{F}(\boldsymbol{v}) \in \mathbf{R}^N$ in the following equation:

$$M\ddot{\bar{\boldsymbol{v}}}(t) + C\dot{\bar{\boldsymbol{v}}}(t) + \boldsymbol{F}(\bar{\boldsymbol{v}}(t)) = 0,$$

where, $M \in \mathbf{R}^{N\times N}$ is the mass matrix; $C \in \mathbf{R}^{N\times N}$ is the damping matrix; $\boldsymbol{F}(\cdot)$ is the nonlinear stiffness vector; $\{\ddot{\bar{v}}_i(t)\}^{\mathrm{T}} = \ddot{\bar{\boldsymbol{v}}}(t) \in \mathbf{R}^N$ is normalised acceleration; $\{\dot{\bar{v}}_i(t)\}^{\mathrm{T}} = \dot{\bar{\boldsymbol{v}}}(t) \in \mathbf{R}^N$ is the velocity; $\{\bar{v}_i(t)\}^{\mathrm{T}} = \bar{\boldsymbol{v}}(t) \in \mathbf{R}^N$ is the normalised displacement and N is the total number of degrees of freedom in the system. If the mass and damping in this system are given as independent uniform variables $m_i = m, c_i = c,\ (i = 1, \cdots, n)$, then we obtain the equation for the nodal variables $\ddot{\bar{v}}_1(t), \dot{\bar{v}}_1(t), \bar{v}_1(t)$ and this gives for the displacement $\bar{v}_1(t)$ for node 1 as follows:

$$m\ddot{\bar{v}}_1(t) + c\dot{\bar{v}}_1(t) + (\beta\mathcal{F}_1(\bar{v}_1) - f) = 0, \tag{41}$$

dividing each term by m, we obtain the following equation

$$\ddot{\bar{v}}_1(t) + c'\dot{\bar{v}}_1(t) + \beta'\mathcal{F}_1(\bar{v}_1(t)) = f'(t), \tag{42}$$

where $c' = c/m$, $\beta' = \beta/m$ and $f' = f/m$ (and includes both the primary path and the bifurcation loads), $f'(t)$ depends on time as the load control parameter. If the value of the damping parameter c' is small, the system response appears as vibration motion analogous to a molecular model.

5 Remarks

This paper clearly shows that there are different bifurcation paths and a primary nonlinear equilibrium path, based on a theoretical solution approach. And there is a hill-top bifurcation point or there are multiple bifurcation equilibrium paths through two BPs. This nonlinear phenomena appears to be folding behaviour that limits the holding supports in a real structure like an umbrella. In future, we will try to confirm this nonlinear strange behaviour experimentally. If you have any ideas about how to do this under static and dynamic conditions, please let us know as it can be collaborative research for academic work.

References

[1] Ario, I., (2004) Homoclinic bifurcation and chaos attractor in elastic two-bar truss. *Int. J. Non-Linear Mechanics*, Vol. 39(4), 605-617.

[2] I. Ario and A. Watson, (2007) Dynamic folding analysis for multi-folding structures under impact loading, *Int. J. of Sound and Vibration*, 308/3-5 (2007) 591-598.

[3] I. Ario and A. Watson, Structural Stability of Multi-Folding Structures with Contact Problem *Int. J. of Sound and Vibration*, 324 (2009) 263-282.

[4] J. M.T . Thompson and G. W. Hunt, *A general theory of elastic stability*, London: Wiley, 1973.

[5] Z. P. Bažant and L. Cedolin, Stability of Structures, Elastic, Inelastic, Fracture, and Damage Theories, Oxford Engineering Science Series, 1990.

[6] I. Ario, Homoclinic bifurcation and chaos attractor in elastic two-bar truss, *Int. J. Non-Linear Mechanics*, 39(4) (2004) 605-617.

[7] I. Ario and M. Nakazawa, Nonlinear Dynamics Behaviour of Multi-Folding Microstructure Systems based on Origami Skill, *Int. J. Non-Linear Mechanics*, accept.